PERGAMON

Journal of Structural Geology 23 (2001) 923–939

JOURNAL OF STRUCTURAL GEOLOGY

www.elsevier.nl/locate/jstrugeo

High-resolution compositional mapping of matrix phases: implications for mass transfer during crenulation cleavage development in the Moretown Formation, western Massachusetts

M.L. Williams*, K.E. Scheltema, M.J. Jercinovic

Department of Geosciences, University of Massachusetts, Amherst, MA 01003-5820, USA

Received 14 January 1999; accepted 11 August 2000

Abstract

High-resolution compositional maps provide a new tool for investigating mass transfer during cleavage formation. The Moretown Formation of western Massachusetts contains a well-developed crenulation cleavage with alternating mica-rich crenulation limbs and mica-poor crenulation hinges. Compositional mapping shows two generations of plagioclase, the second of which was synchronous with the crenulation cleavage. A significant amount of the syn-crenulation plagioclase (10–20% modally) grew in hinge domains. A small amount of syn-crenulation plagioclase (~1%) and a large amount of phengitic muscovite grew in limb domains. The maps also show that uncrenulated domains experienced mass transfer and reactivation of older cleavages, and thus cannot be used as 'undeformed' reference domains for comparison with crenulated regions. Compositional mapping facilitates a new degree of integration between petrologic and structural analysis. Knowledge of the structural context of compositional domains allows better selection of phases and compositions for interpreting metamorphic reactions and linking metamorphism to deformational stages. Knowledge of syntectonic reactions provides new insights into mass transfer and volume change during deformation. In the Moretown Formation, plagioclase- and phengite-producing reactions play a large role in controlling the nature and magnitude of mass transfer, but microstructures control the location of reactants and products within the evolving fabric.

1. Introduction

Crenulation cleavage, consisting of spaced mica-rich (M) and quartz–feldspar-rich (QF) domains (Fig. 1), is the most common type of cleavage in multiply deformed rocks (Borradaile et al., 1982; Mancktelow, 1994). The association between spaced cleavage and millimeter-scale folding has long been recognized (Cosgrove, 1976; Gray, 1977a), and most workers agree that the development of mica-rich domains probably involves the dissolution and removal of large amounts of material from microfold limbs (Gray, 1977b; Marlow and Etheridge, 1977). However, the site of deposition and the driving forces for the transfer of this material are less certain (Mancktelow, 1994). Two end-member hypotheses might be considered. A significant proportion of the dissolved material might be removed from the system (i.e. bulk volume loss). If so, the QF domains may be only minimally affected by the cleavage forming process, and thus they may represent windows to an earlier stage in the deformational and microstructural history (see Bell et al., 1986). Also, unless the material removed is similar in composition to the whole rock, the bulk composition after cleavage formation may be quite different from that of the protolith.

Alternatively, much of the dissolved material may be deposited locally in crenulation hinges, i.e. QF domains (Gray and Durney, 1979; Mancktelow, 1994). If so, the bulk composition of the rock could be similar to that of the protolith, but the fact that the crenulation hinge domains are generally dominated by an earlier fabric (Fig. 1) would suggest that it is possible to add material to these domains without disrupting the earlier folded fabric. This has implications for textural interpretations of other rocks where similar additions of material may also go unnoticed.

The purpose of this paper is to report the results of high-resolution compositional mapping of crenulation cleavage domains and the implications for mass transfer during cleavage formation. Compositional maps, collected using wavelength dispersive spectrometers on the electron microprobe, can depict the geometry of subtle compositional variations in minerals. The results presented here come from the Moretown Formation of western Massachusetts. We have found that the compositions of minerals that grew during

* Corresponding author. Fax: +1-413-545-1200.
E-mail address: mlw@geo.umass.edu (M.L. Williams).

0191-8141/01/$ - see front matter
PII: S0191-8141(00)00164-4

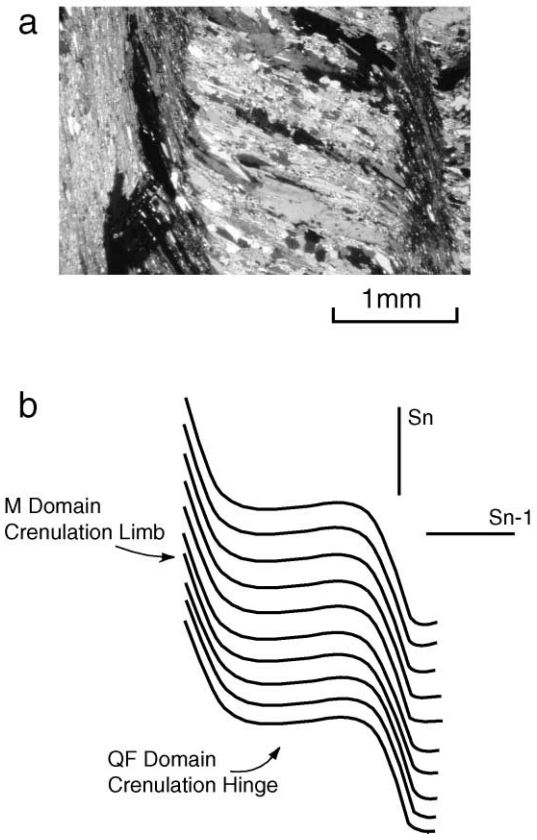

Fig. 1. Photomicrograph (a) and sketch (b) of crenulation cleavage microlithons. M domains (crenulation limbs) are dominated by muscovite with minor biotite, ilmenite, and chlorite. QF domains (crenulation hinges) have muscovite, biotite, quartz, plagioclase, ilmenite, and chlorite with subequal ratios of muscovite + biotite to quartz + plagioclase.

the development of crenulation cleavage are distinct from that of pre-cleavage minerals. Thus, compositional maps of matrix domains provide a means of identifying the sites of new mineral growth, and provide a new tool for tracing and quantifying mass transfer during cleavage formation. Our results show that, at least in the Moretown Formation, cleavage formation is not simply the result of deformation-induced dissolution and precipitation, but instead, it results from the mutually reinforcing interaction of metamorphic reactions and micro-deformational processes.

2. Background

2.1. Mass transfer and cleavage formation

Numerous studies have investigated mass transfer during cleavage formation (Gray and Durney, 1979; Beutner and Charles, 1985; Waldron and Sandiford, 1988; Bell and Cuff, 1989; Wright and Henderson, 1992; Mancktelow, 1994; Goldstein et al., 1995; Tan et al., 1995; Erslev, 1998). These can be broken into two broad groups, microchemical studies and microtextural or microfabric studies. Particularly in studies of cleavages developed at low and medium metamorphic grades, the two types have reached rather different conclusions about cleavage-forming processes. Textural studies and strain studies have emphasized dissolution and removal of material from cleavage domains (Marlow and Etheridge, 1977; Bell et al., 1986; Wright and Henderson, 1992; Goldstein et al., 1995). The lack of obvious sinks for the dissolved material and constraints from strain measurements tend to suggest that dissolved components have been removed from the system. For example, volume loss in some slates has been interpreted to be as large as 50% (Beutner and Charles, 1985; Wright and Henderson, 1992; Goldstein et al., 1998) and similar values could be interpreted for crenulation cleavages (Bell et al., 1986). In contrast, geochemical studies of low-grade slatey cleavage and of crenulation cleavage in higher-grade rocks have generally not found significant bulk compositional differences between high- and low-strain (crenulated and uncrenulated) domains, and thus find little evidence for significant volume loss (Mancktelow, 1994; Saha, 1998; cf. Erslev, 1998). Certainly, if large losses were dominated by SiO_2, they would be readily apparent in geochemical comparisons. However, questions about the 'undeformed' (by the event under consideration) nature of uncrenulated reference domains and suggestions that mass transfer may involve multiple chemical components lead to persistent questions about the geochemical results.

2.2. Moretown Formation

The Moretown Formation is one of a series of N–S-trending lithologic belts of Cambrian to Ordovician rocks that occur east of the Berkshire massif in western New England (Stanley et al., 1984; Stanley and Hatch, 1985; Robinson et al., 1993; Thompson et al., 1993). In western Massachusetts, the rocks are collectively known as the Rowe–Hawley Belt and consist of the Rowe, Hawley, and Moretown Formations (Stanley and Ratcliff, 1985). They are interpreted to be the remains of an accretionary prism (Rowe Formation), forearc basin (Moretown Formation), and slices of arc-related igneous rocks (Hawley Formation) that were thrust onto Laurentia during the Taconic orogeny (Stanley and Ratcliff, 1985; Robinson et al., 1993). Contacts between and within the units have been considered to be Taconic thrusts, but many have almost certainly been reactivated during the Acadian orogeny (Stanley and Ratcliff, 1985; Karabinos and Williamson, 1994). Deposition in the Moretown Formation began before approximately 494 Ma based on the age of cross-cutting dikes in Vermont (Ratcliffe et al., 1997). In Massachusetts, the Moretown Formation is cut by the 479 Ma Hallockville Pond gneiss (Karabinos and Williamson, 1994).

The Moretown Formation is characterized by interbedded schist and quartzite to greywacke layers ranging in thickness from centimeters to meters. Massive layers, locally described as pinstripe feldspathic granofels (or granulite)

and layers interpreted as metamorphosed volcanics have been described (Hatch et al., 1968; Hatch, 1969; Robinson et al., 1993). Amphibolite layers and lenses are common, and many are discordant to the dominant layering. Metamorphic conditions reached upper greenschist to amphibolite facies (Florence et al., 1989), and many rocks show evidence of a polymetamorphic or protracted metamorphic history. Assemblages include combinations of garnet, biotite, muscovite, chlorite, plagioclase, quartz, ilmenite with trace amounts of apatite and epidote.

The Moretown Formation provides an excellent example of small-scale folding and crenulation cleavage development. Gradients occur from uncrenulated domains, through domains with classic crenulation cleavage, to schistose high-strain domains. Individual compositional layers can be traced across the fabric transitions. The samples investigated here were collected from outcrops on Rt. 9 in West Cummington, Massachusetts. These outcrops are dominated by upright, open to tight folds with amplitudes and wavelengths on the order of 10 cm to several meters (Fig. 2). These upright folds represent at least third-generation (F_3) structures. They fold a strong, relatively homogeneous cleavage (S_2), which can locally be seen to represent a highly evolved spaced crenulation cleavage, having formed by the folding of an earlier foliation (S_1). Although the presence of earlier S_1 and S_2 cleavages suggests a complex structural history, the two fabrics combine to create a continuous planar fabric with regular compositional variation that provides excellent marker layers for investigating F_3 folding and cleavage formation.

F_3 folds in the Moretown Formation display spectacular crenulation cleavage. The cleavage is absent or only weakly developed on fold limbs, and becomes increasingly intense toward the fold hinges (Fig. 2). Where the cleavage is best developed, the mica-rich M domains consist almost entirely of muscovite, biotite, and ilmenite, oriented parallel to the axial surfaces of the F_3 folds. The intervening QF domains contain quartz, plagioclase, garnet, biotite, muscovite, and ilmenite, all aligned with the folded S_2 surfaces. Typical of many crenulated rocks, garnet porphyroblasts are restricted to the QF domains (Bell et al., 1986; Williams, 1994; Scheltema and Williams, 1999). They range in size from 0.1 to 3 mm and many have distinct core and rim domains (Scheltema and Williams, 1999). Cores dominate the crystals and contain spiral-shaped inclusion trails with 90–450° of apparent rotation. They are associated with triangular quartz- and feldspar-rich pressure shadows (strain shadows) that are aligned with the S_2 cleavage and folded by the F_3 folds. The fact that the strain shadows and the inclusion trails are generally aligned with the S_2 cleavage indicates that the bulk of the garnet crystals, the cores, grew before and during the S_2-forming event. Most garnet crystals also have narrow rims that overgrow the S_2 strain shadows and the early stages of the S_3 crenulation cleavage (Scheltema and Williams, 1999). Thus, the latest phase of garnet growth is interpreted to be contemporaneous with the S_3 cleavage.

2.3. Geochemical analysis

Scheltema (1996) carried out a geochemically based analysis of volume change using a suite of samples from the fabric gradient in the Moretown Formation sample (MT-1) shown in Fig. 2. Whole rock compositions were compared using the method of Gresens (1967) as modified by Potdevine and Marquer (1987) and Mancktelow (1994). The results were in accordance with the results of numerous other studies; geochemical data would permit only small amounts (0–12%) of volume loss even when comparing the strongest crenulation cleavages to the weakest (Fig. 2b). Slightly greater amounts were interpreted when the high-strain, shear zone domains were included, but these do not involve simple crenulation cleavages. These estimates are well below virtually all texturally based estimates of the amount of material dissolved from crenulation cleavage domains (i.e. 30–50%). The contrast between interpretations of large amounts of volume loss as suggested by microstructural analysis and virtually no volume loss as indicated by geochemical analysis serves as a primary motivation for the present study (see also Erslev, 1998).

3. Methods

Compositional mapping of metamorphic and igneous minerals is routinely carried out in petrologic studies (Pattison and Bégin, 1994; Spear and Kohn, 1996). To create compositional maps of large areas (one to tens of millimeters on a side), wavelength dispersive spectrometers are placed at the peak position of elements of interest and the stage is moved through a square grid of points (i.e. stage scanning). For smaller areas, typically hundreds of microns on a side, the stage is held fixed and the electron beam is moved through a grid of points (beam scanning). For this study, compositional mapping was carried out on the Cameca SX50 electron microprobe at the University of Massachusetts. Most maps involve a count time of 0.1 s and a current of 100 nA, but for all maps the value of the product of beam current and count time was maintained at 10. Three general scales of maps were collected. The largest two involved stage scanning and the smallest involved beam scanning. Large-area maps range from 0.5 to 1 cm on a side, and generally have 1024 steps with a 5–10 μm step size. Medium-scale maps are approximately 1 mm squares, typically 512 steps per line with a 2 μm step size. Small-scale maps are typically 256 μm squares with 512 steps and 0.5 μm step size per side.

Image analysis was carried out using the public domain software, NIH Image. In general, maps were processed independently to maximize contrast (i.e. colors were not specifically indexed to composition). Large-area high-resolution maps were assembled from multiple, small-scale

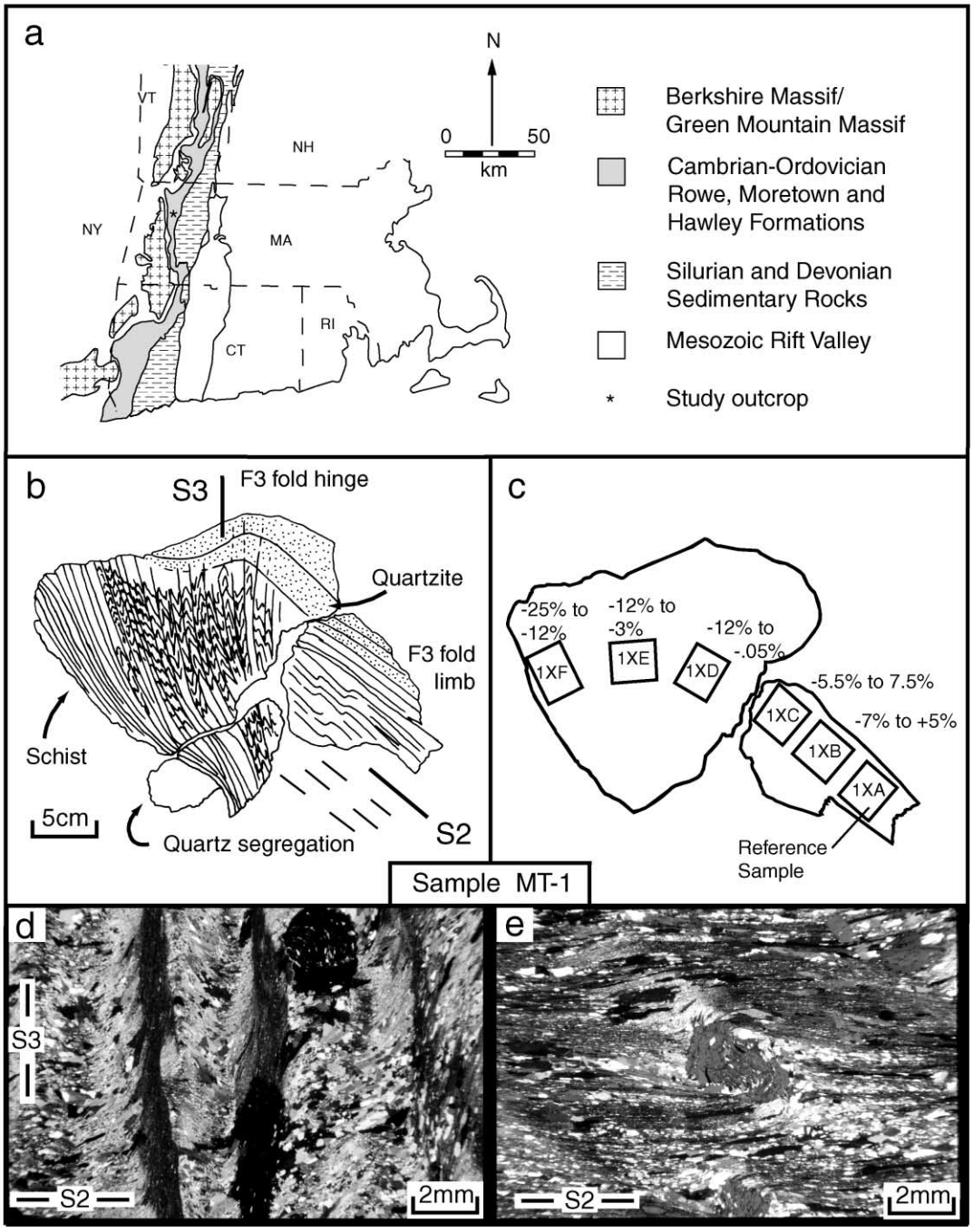

Fig. 2. (a) Generalized geologic map showing major lithotectonic units in western New England. The Rowe–Hawley zone, including the Moretown Formation, is shown in gray (see text for discussion). (b) Sketch of Moretown Formation sample MT-1, collected on Rt. 9 in West Cummington, MA. (c) Location of samples used for whole rock analysis (Scheltema, 1996). Samples, roughly cubes, span the transition from uncrenulated limb to crenulated hinge region of fold. Volume change relative to the reference sample in the uncrenulated limb may be as much as 12% during crenulation cleavage formation. Larger volume loss (~25%) is observed near a quartz segregation where S_3 is a strong schistose cleavage. (d) Photomicrograph of typical crenulation cleavage from hinge domain of sample MT-1. (e) Photomicrograph of uncrenulated S_2 cleavage in limb domain of sample MT-1.

high-resolution maps that were collected from adjacent areas under identical microprobe conditions. The raw images were combined before processing and then processed together. Mineral modes and percent area measurements were also made using the NIH Image thresholding and density slice tools (see below).

All of the compositional maps presented come from a single slab sample of the Moretown Formation, MT-1, oriented normal to the F_3 fold axis. The sample contains an asymmetric fold with three structural domains: a fold limb domain with little S_3 crenulation cleavage, a fold hinge domain with well-developed crenulation cleavage,

and a third domain with intense, schistose S_3 cleavage that borders a large quartz segregation (Fig. 2). This particular fold sample was selected for compositional mapping because the quantitative geochemical analyses (Scheltema, 1996) were done on an adjacent slab of the same sample (Fig. 2b). This study focuses on the crenulated hinge and uncrenulated limb domains, and is in some ways modeled after the studies of Marlow and Etheridge (1977) and Mancktelow (1994) in which textural and compositional data were compared from crenulated to uncrenulated domains. However, these previous studies primarily involved comparisons of microstructure and bulk composition. In this study, we use high-resolution compositional images from different structural domains to investigate the timing and nature of mass transfer during cleavage formation.

Because the fold sample has multiple scales of structural domains, nomenclature can be confusing. For this study, macroscopic F_3 fold domains of sample MT-1 will be referred to as 'fold limb' and 'fold hinge' domains. Within the fold hinge domains, small-scale microfold domains (crenulations) will be referred to as crenulation hinge and crenulation limb domains. The terms mica-rich or 'M' domains and mica-poor or 'QF' domains will be used to refer to the mineralogically distinct cleavage microlithons, which generally correspond to the crenulation limbs and hinges, respectively (Figs. 1 and 2) (after Marlow and Etheridge, 1977).

4. Results

4.1. Strongly crenulated fold hinge domains—sample MT-1

Hinge regions of macroscopic folds are dominated by crenulation cleavage (Fig. 2). Fig. 3 shows a single crenulation microfold from which several compositional maps have been collected. The mica-poor, QF domains (crenulation hinges) consist of quartz, plagioclase, biotite, muscovite, and ilmenite with scattered garnet porphyroblasts (Fig. 3a, b; Table 1). The ratio of muscovite + biotite to quartz + feldspar (M:QF) is slightly greater than unity; that is, QF domains have subequal amounts of mica and quartz + feldspar (note: quartz and feldspar are commonly combined in microstructural studies because the lack of twinning in feldspar makes them difficult to distinguish on a bulk scale). M domains (crenulation limbs) are dominated by muscovite; M:QF ratios in these domains range from 7 to more than 25 (Table 1). Biotite is significantly coarser than muscovite and is only slightly more abundant in M than QF domains. Although all M domains have greater modal muscovite than QF domains, significant variation occurs from one M domain to another even within a single thin section. Mg Kα compositional maps highlight the location and distribution of biotite and chlorite (Fig. 3c). Because these minerals tend to be present in both crenulation hinge and crenulation limb domains, the Mg maps are particularly useful for showing the general microstructure. The maps also show that some biotite books are bent and deformed whereas others are straight and cross-cut the folded foliation.

Ca Kα compositional maps (Fig. 3d) show the composition and distribution of plagioclase. Except for a small amount of apatite, plagioclase is the only Ca-bearing matrix phase (epidote occurs locally as inclusions in garnet). Because of the similar optical appearance of quartz and feldspar, many workers have tended to focus on the abundance of quartz in QF vs M domains, so much so that in some reports these domains are referred to as Q rather than QF domains. However, in the Moretown Formation, QF domains all have a significantly greater percentage of plagioclase than M domains, suggesting that plagioclase, in addition to quartz, has either been removed from the crenulation limbs or added to the crenulation hinges or both. Thus, although other studies have focused on quartz mobility, Fig. 3(d) documents that plagioclase solution and precipitation is an important part of the cleavage-forming process in the Moretown Formation (see also Erslev, 1998; Saha, 1998).

Fig. 4(a) is a high-resolution optical image of a single QF, crenulation hinge domain from within Fig. 3. Fig. 4 shows small-area, Ca Kα maps of individual plagioclase grains from crenulation hinge (QF) domains and crenulation limb (M) domains, respectively. All of the compositional maps show plagioclase crystals with Ca-poor cores surrounded by Ca-richer rims. In crenulation hinges, the cores have a distinct elongation with aspect ratios of 3:1 or more, and are aligned with the folded S_2 cleavage (Fig. 4b, d). Overgrowths are more equant but tend to have the same S_2-parallel dimensional preferred orientation. In crenulation limbs, the composite feldspar grains are significantly smaller than they are in hinges (Fig. 4c). Ca-rich overgrowths have large aspect ratios and are aligned with the new S_3 crenulation cleavage. Some overgrowths are fibrous and others are fractured and extended along S_3. Grain cores tend to have smaller aspect ratios compared to those in crenulation hinges, and may have been partially dissolved or resorbed during the early stages of cleavage formation. In some areas, particularly in the transition between crenulation hinges and limbs, the cores define a foliation at a distinct angle to that defined by the overgrowths (Fig. 4d). Although in these localities the matrix fabric is generally dominated by the new S_3 orientation, the cores preserve an earlier orientation of the folded S_2 cleavage.

As discussed below, similar plagioclase core and rim compositions occur in all structural settings. Cores are approximately An_{03} (albite) and rims are $An_{14–16}$ (oligoclase, Table 2). The alignment of plagioclase overgrowths with S_3 crenulation cleavage and the presence of fibrous, S_3-parallel overgrowths suggests that the overgrowths were produced during crenulation development. The cores apparently represent relict grains that were stable during the

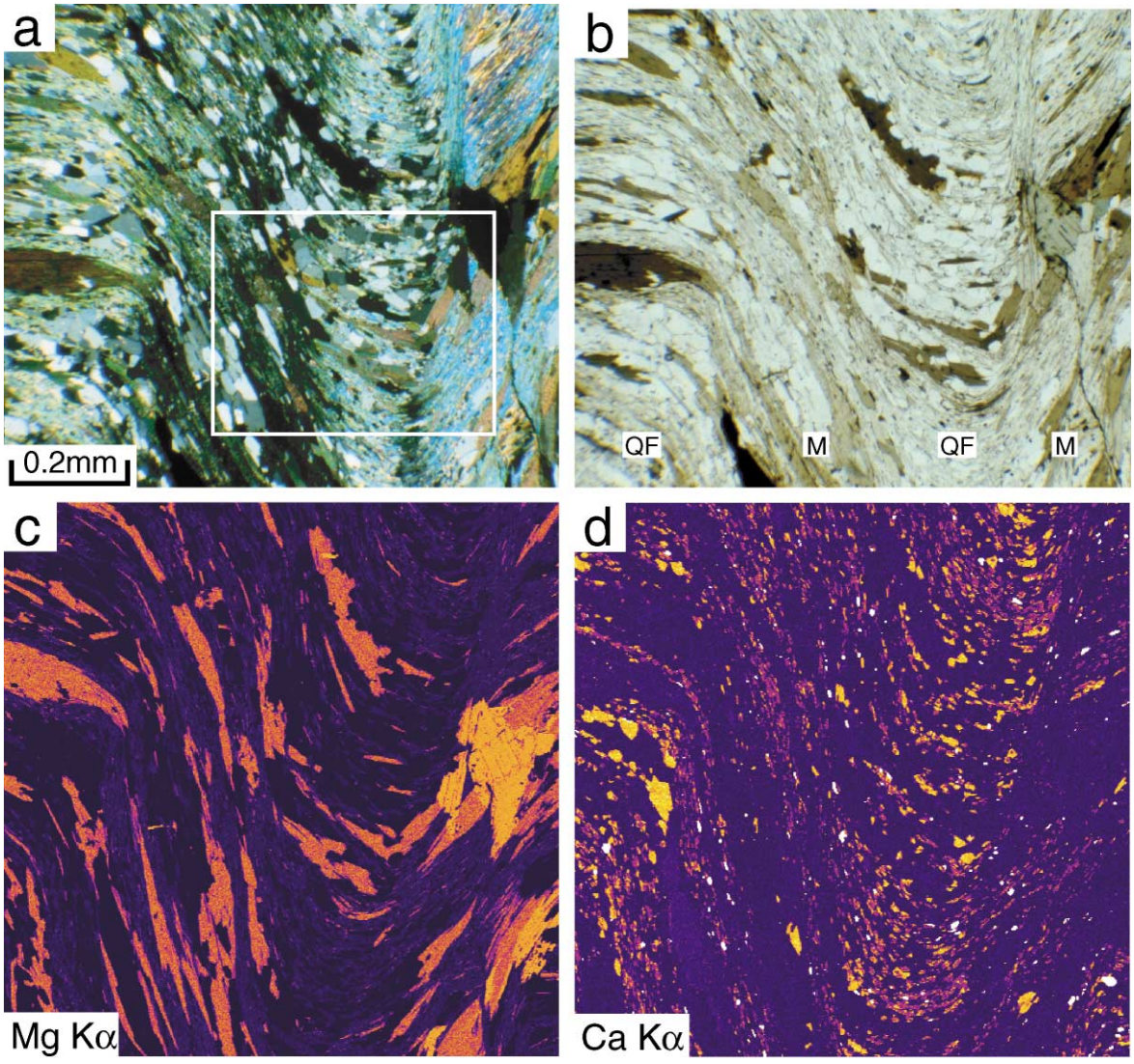

Fig. 3. Photomicrograph (a—crossed polars; b—uncrossed polars) of a single crenulation microfold from hinge of sample MT-1. From left to right, sample shows four alternating domains: QF–M–QF–M. Box shows location of Fig. 4. (c) Mg Kα compositional map of same area as (a), (b) (orange = chlorite; red = biotite). (d) Ca Kα compositional map of same area as (a), (b) (yellow-orange = plagioclase; purple = albite). See text for discussion.

Table 1
Modes[a] of major phases in selected samples of Moretown Formation sample MT-1

	MT-1-A Fold limb	MT-1-G fold hinge							
		QF domains				M domains			
		1	2	3	Avg	1	2	3	Avg
Chlorite	4.5	0.7	0.3	1.3	0.8	0.0	0.4	5.2	1.9
Biotite	15.1	20.2	6.3	10.9	12.5	10.8	3.1	7.6	7.2
Muscovite	51.4	44.2	37.7	55.5	45.8	82.9	81.1	80.0	81.3
Quartz	19.5	16.3	40.2	23.5	26.6	2.1	8.6	2.6	4.4
Plagioclase	8.4	17.6	14.4	7.9	13.3	1.7	3.6	1.6	2.3
Ilm. & other	1.2	0.9	1.1	1.0	1.0	2.5	3.1	3.0	2.9
M:QF ratio[b]	2.4	1.9	0.8	2.1	1.5	24.7	6.9	20.9	13.1

[a] Modes determined using compositional maps and density slice technique (see text for discussion).
[b] M:QF = ratio of muscovite + biotite to quartz + feldspar.

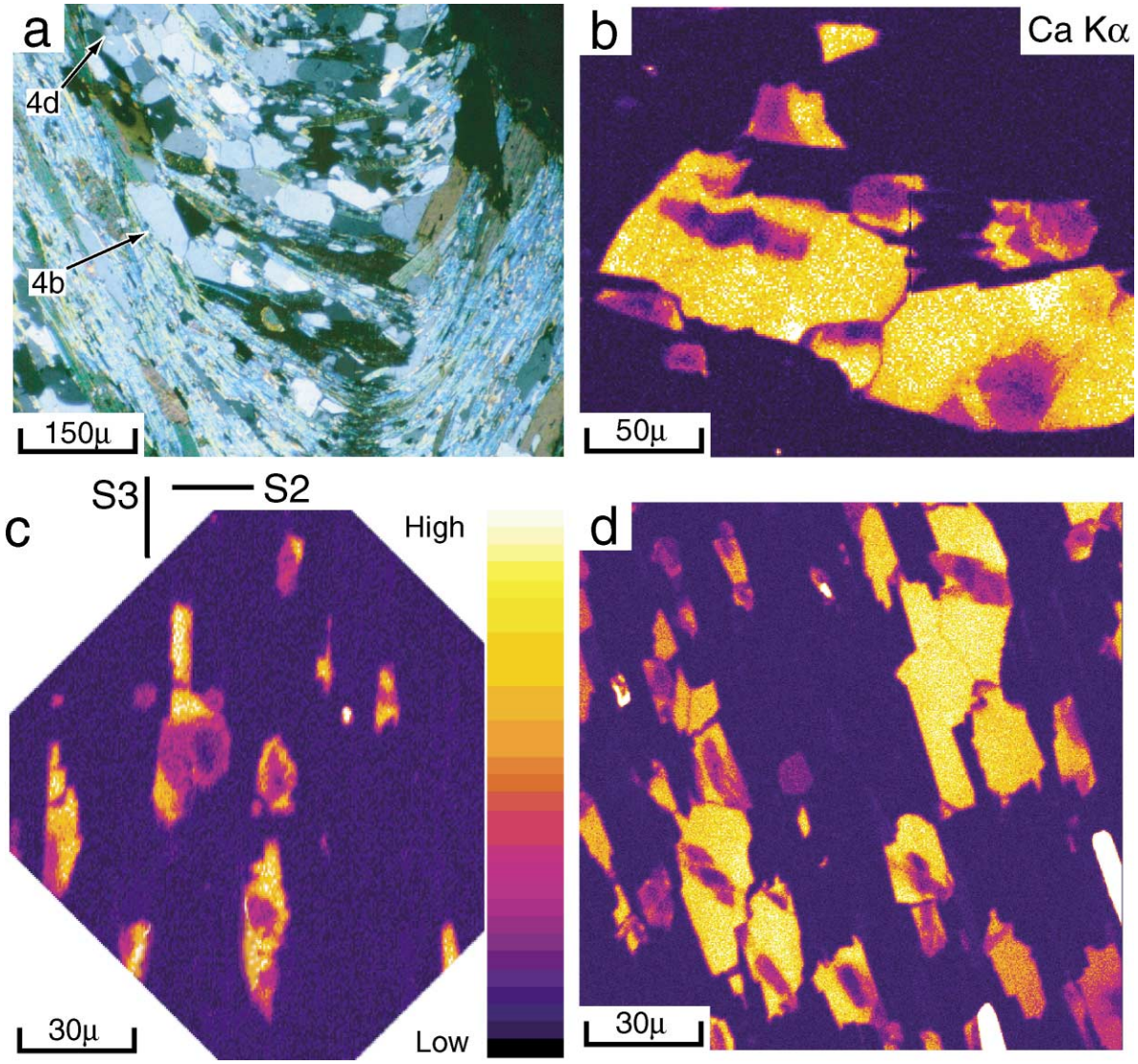

Fig. 4. (a) Photomicrograph of one crenulation hinge, QF domain from Fig. 3. Arrows indicate grains mapped in (b) and (d). (b) Ca Kα map of plagioclase grains from QF domain (purple = An_{03}; yellow = $An_{14–16}$). (c) Ca Kα map of plagioclase grains from M domain, just to the left of (a). (d) Ca Kα map of plagioclase grains from transition between M and QF domains. (b)–(d) Fixed stage, beam-scan compositional maps.

development of the earlier S_2 fabric. Thus, the Ca-richer plagioclase can be used as a marker or tracer of new mineral growth during crenulation cleavage development. It occurs predominantly in crenulation hinge domains where it tends to mimic and preserve the old folded S_2 cleavage. In crenulation limb domains, the relatively minimal second-generation plagioclase is strongly aligned with S_3 and is an important component of the new fabric.

4.2. Uncrenulated domains

Limb domains of macroscopic folds are dominated by S_2 cleavage (Fig. 2e). If present at all, the F_3 (crenulation) event is characterized by a gentle warping of the S_2 fabric. Ca Kα compositional maps from the uncrenulated region of sample MT-1 are shown in Fig. 5. The largest map area includes a garnet porphyroblast with distinct quartz- and plagioclase-rich strain shadow domains (Fig. 5a). As in the crenulated domains, there are two distinct plagioclase compositions, low-Ca cores and Ca-richer overgrowths (Fig. 5b). Although most grains are tens to hundreds of microns in diameter, several large grains, compositionally similar to the overgrowths (orange-colored grains), are also present (Fig. 5b). The second-generation plagioclase is primarily concentrated in the garnet strain shadows, but some of the Ca-richer plagioclase is also dispersed throughout the matrix.

High-resolution Ca Kα images (Fig. 5c, d) show that overgrowth plagioclase primarily occurs as needles, fibers, and strain shadows aligned with the S_2 cleavage. Many of the strain shadows are asymmetric with respect to their host plagioclase, and if interpreted to be sigma-style tails

Table 2
Selected mineral analyses from Moretown Formation sample MT-1

	Garnet		Plagioclase		Muscovite		Biotite	Chlorite
	Core	Rim	Core	Rim	Normal	Phengitic		
FeO	23.79	35.02	0.07	0.02	1.76	2.39	20.84	25.99
MgO	0.99	2.46	0.00	0.00	0.94	1.60	9.47	13.90
MnO	10.25	0.72	0.00	0.00	0.00	0.00	0.10	0.08
CaO	6.27	3.18	0.76	3.07	0.02	0.00	0.00	0.00
Na_2O	0.00	0.00	11.78	10.31	1.46	0.78	0.10	0.03
K_2O	0.00	0.00	0.06	0.05	9.02	9.51	9.31	0.00
TiO_2	0.16	0.05	0.00	0.00	0.26	0.41	1.95	0.06
Fe_2O_3	0.00	0.00	0.00	0.00	0.00	0.00	0.00	0.00
H_2O	0.00	0.00	0.00	0.00	0.00	0.00	0.00	0.00
Al_2O_3	21.05	21.62	20.39	22.30	35.01	32.28	17.51	22.18
SiO_2	36.49	37.16	66.23	63.29	46.72	47.32	35.74	23.49
Total	99.00	100.22	99.29	99.04	95.20	94.29	95.01	85.73
Cations								
Fe^{2+}	1.622	2.349	0.003	0.001	0.098	0.135	1.340	1.856
Mg	0.120	0.294	0.000	0.000	0.093	0.160	1.085	1.769
Mn	0.708	0.049	0.000	0.000	0.000	0.000	0.006	0.006
Ca	0.548	0.274	0.036	0.147	0.002	0.000	0.000	0.000
Na	0.000	0.000	1.010	0.892	0.188	0.102	0.016	0.005
K	0.000	0.000	0.003	0.003	0.764	0.816	0.913	0.000
Ti	0.010	0.003	0.000	0.000	0.013	0.021	0.113	0.004
Fe3	0.000	0.000	0.000	0.000	0.000	0.000	0.000	0.000
Fe^{3+}	0.000	0.000	0.000	0.000	0.000	0.000	0.000	0.000
Al	2.023	2.044	1.063	1.173	2.738	2.559	1.587	2.232
Si	2.975	2.981	2.930	2.823	3.070	3.183	2.749	2.006
Total	8.004	7.994	5.045	5.038	6.964	6.976	7.809	7.877
End members								
Alm	0.541	0.792						
Py	0.040	0.099						
Spess	0.236	0.017						
Gros	0.183	0.092						
An			0.034	0.140				
Ab			0.962	0.849				
Or			0.003	0.002				

(Passchier and Trouw, 1996) they consistently suggest top-west shearing or thrusting on the S_2 cleavage. The compositions of plagioclase cores and rims are identical to those seen in the crenulated fold hinge domains, i.e. albite cores with oligoclase rims. We interpret the overgrowths to represent syn-D_3 plagioclase growth. The fact that the overgrowths are fibrous, asymmetric, and locally broken and extended indicates active shearing along the S_2 cleavage during overgrowth formation, suggesting that D_3 deformation was characterized by reactivation of the S_2 cleavage in the fold limb domains. Thus, uncrenulated domains cannot be taken as undeformed domains for textural and geochemical comparison with the crenulated domains. Both have experienced deformation during the crenulation forming event and both have undergone the mass transfer processes as indicated by the dissolution of plagioclase cores and the growth of Ca-richer rims.

4.3. Quantitative results

Compositional maps allow rapid and efficient estimation of mineral modes or even the relative abundance of a particular compositional range in zoned minerals. Many image analysis programs, such as NIH Image, allow selection of density slices within the color spectrum of an image. A density slice is a selected range of intensity values that can be assigned a specific color value and distinguished from the rest of the image. For example, within the full spectrum of a Ca Kα image the color range that represents only the overgrowth plagioclase composition (i.e. An_{14-16}) can be selected (Fig. 6a—red color). When several minerals have similar color ranges, images for different elements can be added or subtracted to make a particular color range unique to the mineral of interest. Then, by selecting areas of interest, it is possible to compare the area of the selected density slice to the total area, and thus to estimate the mode of a chosen component.

Using the density slice technique, modes of second-generation plagioclase have been estimated in several structural settings in sample MT-1 (Fig. 6b–d). In samples with strong crenulation cleavage, M domains (crenulation limbs) contain approximately 1% of the Ca-richer, overgrowth

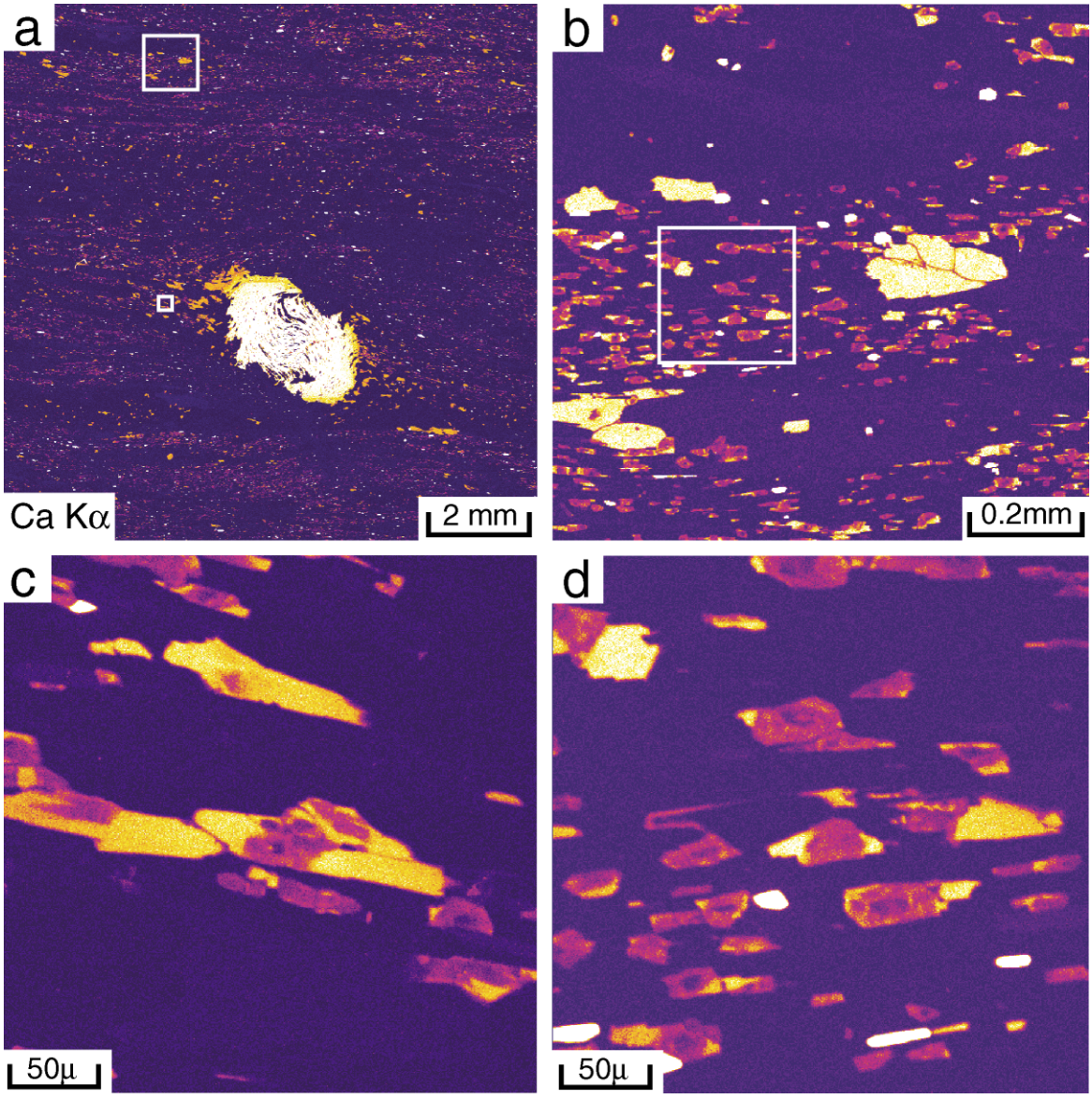

Fig. 5. (a) Large-area Ca Kα map of uncrenulated fold limb domain of sample MT-1 (Fig. 2); white—garnet; yellow—plagioclase. Large box shows area of (b); small box shows area of Fig. 4(c). (b) Ca Kα map of large box in (a). Small plagioclase grains have core compositions of An_{03} (purple) and rim compositions of An_{14-16} (yellow). Composition of large plagioclase grains is the same as rims of small grains, and are large new metamorphic plagioclase grains. (c) Ca Kα map of plagioclase grains from garnet strain shadow (small area in (a)); purple—An_{03}; yellow—An_{14-16}. (d) Close-up Ca Kα map of plagioclase grains in (b) (area shown in box). Note that second-generation plagioclase forms syn-kinematic asymmetric tails on plagioclase cores. (a), (b) Fixed-beam stage-scan compositional maps; (c), (d) fixed-stage, beam-scan compositional maps.

plagioclase whereas QF domains (crenulation hinges) consistently contain greater than 10% Ca-richer plagioclase (Fig. 6b). This emphasizes the conclusion made above that crenulation hinges are favorable sites for plagioclase growth. Even greater amounts of new plagioclase occur adjacent to garnet porphyroblasts in QF domains (Fig. 6c) where modes as high as 30% are common. Many of these enriched zones near porphyroblasts are not apparent as shadows or beards in thin section or hand specimen. Without compositional maps, they might be mistakenly interpreted as low-strain domains dominated by the earlier cleavage; instead, they have been significantly dilated during crenulation development.

As noted, uncrenulated fold limb domains of sample MT-1 also contain the Ca-richer, syn-S_3 plagioclase (Fig. 6d). Typical matrix domains have several percent of Ca-richer plagioclase and porphyroblast shadows have approximately 10%. Measurements generally fall between those of the crenulation limb and hinge domains. It is not clear if the second-generation plagioclase represents material derived locally (i.e. within fold limbs) or more regionally (from crenulated regions), but the results further

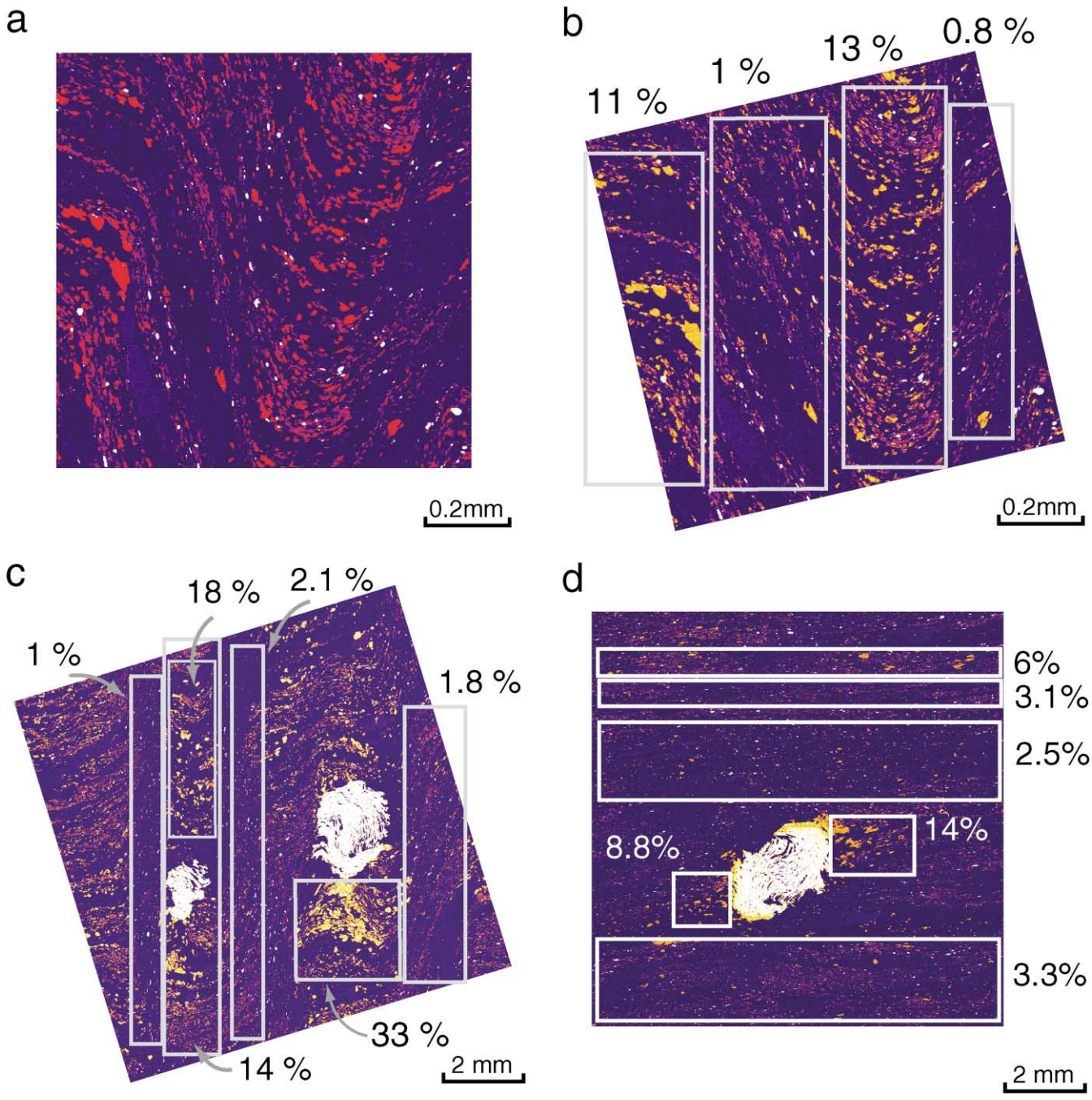

Fig. 6. Quantitative analysis of compositional maps. (a) Compositional map shown in Fig. 3(d) with new plagioclase (An_{14-16}) selected as a density slice (red). (b) Modes of new plagioclase in M and QF domains from sample shown in Fig. 3(d). Modes determined by dividing the number of selected pixels (a) by total number of pixels in selected area. (c) Modes of new plagioclase in M and QF domains from a strongly crenulated region of sample MT-1 with garnet porphyroblasts (white). (d) Modes of new plagioclase in matrix and strain shadow domains in an uncrenulated sample from limb region of sample MT-1 (same map area as Fig. 5a).

emphasize the observation that even though crenulation cleavage has not developed in F_3 fold limbs, the uncrenulated domains have experienced deformation and significant mass transfer during the cleavage forming event.

4.4. Large-scale matrix mapping

For some petrologic and structural questions, it is useful to build large-scale, high-resolution compositional image mosaics of matrix domains. Fig. 7 shows one example from the crenulated hinge region of sample MT-1. The Na Kα compositional map is particularly useful for showing the composition and distribution of muscovite (Fig. 7a). Two compositions of muscovite are present in most samples, a higher-Na, normal muscovite and a lower-Na, phengitic muscovite. In general, phengitic muscovite

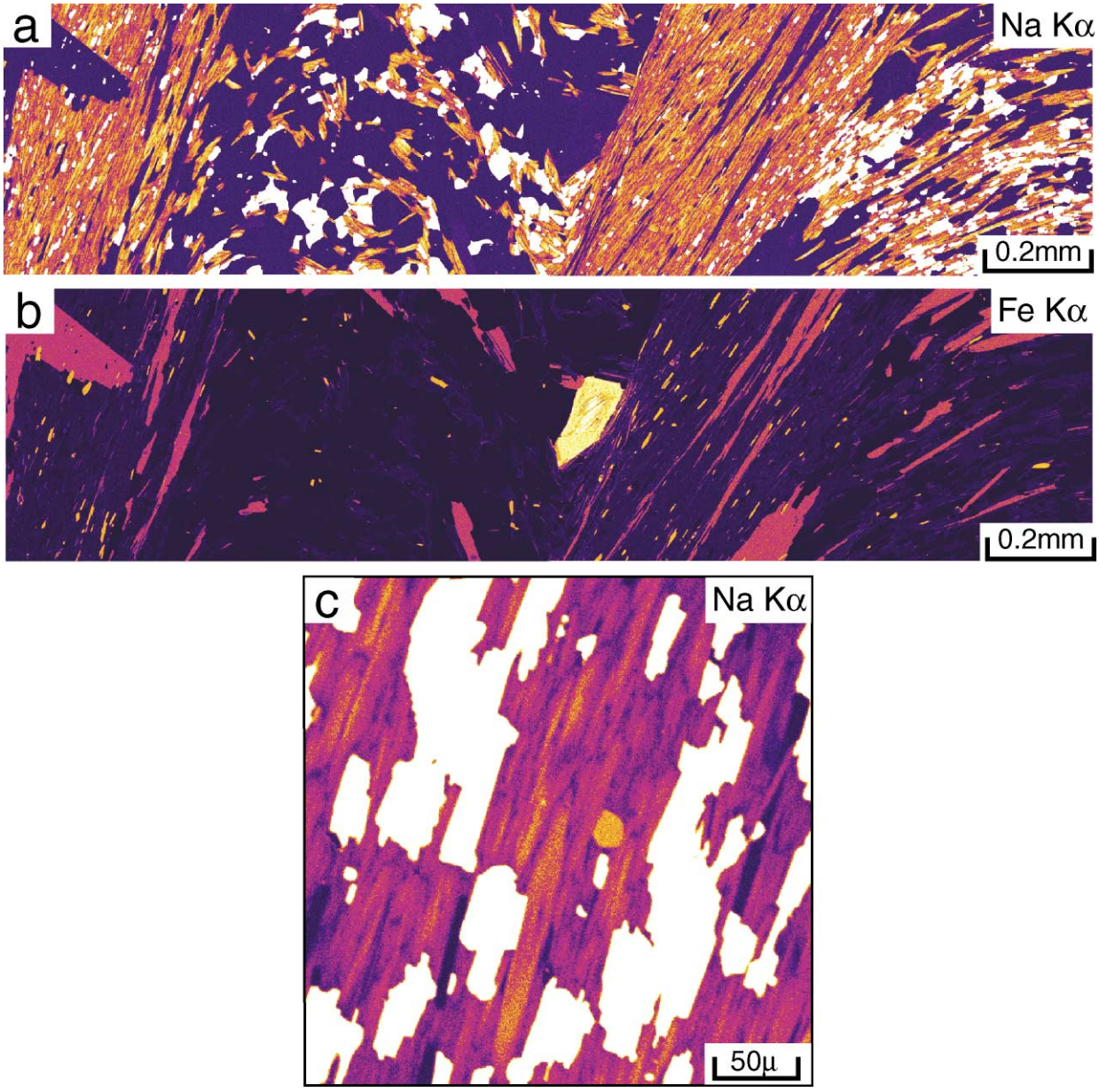

Fig. 7. Large-area mosaics of compositional maps for petrologic and mass balance analysis. Each map constructed from four high-resolution, stage-scan maps (512 × 512 steps; 2 μm per step). (a) Na Kα map of two M domain/QF domain pairs (white—plagioclase; yellow-orange—normal muscovite; purple-orange—phengitic muscovite). (b) Fe Kα map of same area as (a) (yellow—pyrite; orange—ilmenite; red—biotite + chlorite). (c) Close-up Na Kα map from central M domain in (a). Note euhedral muscovite (orange) surrounded by phengitic muscovite (purple-red); white—plagioclase.

surrounds (overgrows?) the high-Na muscovite (Fig. 7c). Although both types of muscovite are present in crenulation hinge and limb domains, the phengite:muscovite ratio is greater in crenulation limbs (M domains), where it is strongly aligned with the new S_3 cleavage. This suggests that phengite grew during the development of the S_3 crenulation cleavage.

Large-area Fe Kα compositional maps are useful for evaluating the distribution of Fe oxides (Fig. 7b). Ilmenite is significantly more abundant in M domains than in QF domains. Ilmenite grains are strongly aligned with the S_3 crenulation cleavage, and locally cut folded micas. Thus, like phengitic muscovite, some of the ilmenite developed during crenulation formation. Much of this new ilmenite is believed to result from the consumption of biotite in metamorphic reactions that were active during the growth of the phengitic muscovite (see below).

Matrix compositional maps such as these provide insight into the timing of metamorphic reactions and their relationship to deformation. They also help to illuminate the crenulation forming processes themselves. Some workers have tended to see crenulation cleavage M domains as relict

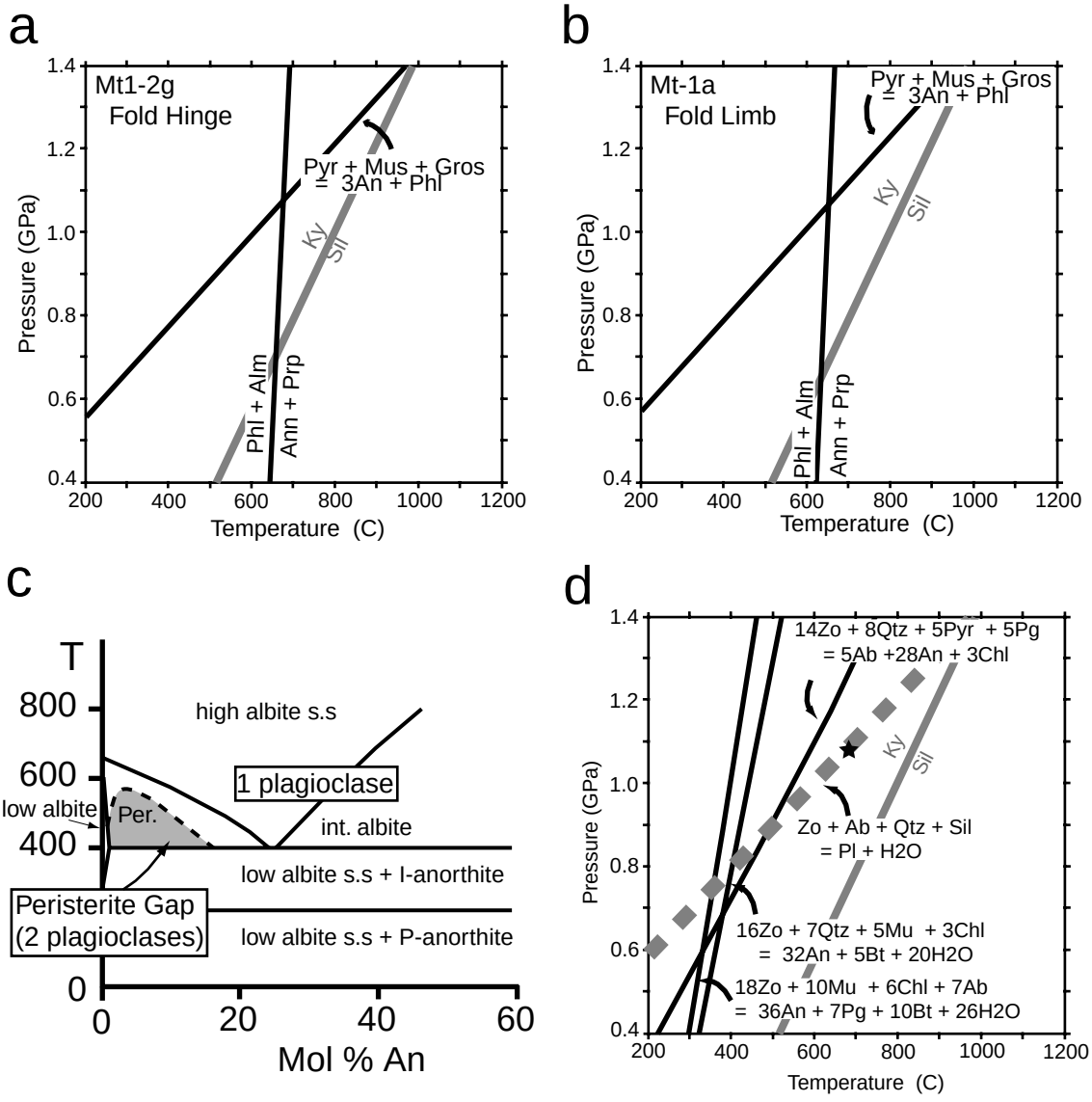

Fig. 8. Petrologic data from Moretown Formation sample MT-1. (a) Equilibria from crenulated fold hinge domain, calculated using the database and software of Berman (1991). Peak conditions are approximately 1.1 GPa, 650°C. (b) Equilibria from uncrenulated fold limb domain. Compositions for calculations (Table 2) based on analyses of 5 garnet crystals and more than 20 muscovite and biotite books from each domain. Independent reactions chosen to correspond to the Grt–Bt thermometer and Grt–Bt–Ms–Qtz barometer. (c) Plagioclase structural and compositional relationships (modified from Smith, 1983). (d) Possible reactions involving zoisite (epidote) consumption and anorthite production. Solid lines are calculated reactions using compositions from sample MT-1 (Table 2) and database of Berman (1991). Dashed line is experimentally determined reaction from Newton (1966). Black star shows peak conditions for sample MT-1. Note: all reactions are consistent with development of metamorphic plagioclase on heating at 1.1 GPa.

domains, that is, domains dominated by components left behind after the dissolution of quartz, feldspar and other phases (see Gray and Durney, 1979; Mancktelow, 1994). However, if ilmenite and phengitic muscovite did indeed develop during D_3, then a significant amount of muscovite grew or was recrystallized during crenulation development. This has important implications for mass transfer studies because the mineral modes in crenulation domains cannot be used to constrain the amount of material removed. They represent dynamic domains that have gained and lost components as governed, at least partially, by syntectonic metamorphic reactions.

4.5. P–T constraints

Tectonic interpretations of deformation fabrics commonly require estimates of *P–T* conditions linked to individual deformation events. A major source of error in such analyses involves the selection of mineral phases and compositions for *P–T* calculations. It is critical to select assemblages and compositions that were in equilibrium during the deformation event of interest. Calculations of metamorphic pressure are critical for tectonic interpretations and many geobarometers are particularly sensitive to garnet and plagioclase composition. Matrix compositional

maps provide timing constraints and a critical link between P–T conditions and deformation fabrics.

As noted above, narrow garnet overgrowths developed during the D_3, crenulation-forming deformation (Scheltema and Williams, 1998). Garnet cores contain S_1 inclusion trails and have syn-S_2 strain shadows suggesting that they developed during D_2. Overgrowths contain sigmoidal S_2 inclusion trails and overgrow the syn-S_2 strain shadows, indicating syn-D_3 growth (Scheltema and Williams, 1999). These observations, combined with timing constraints from matrix mapping (above), suggest that the metamorphic assemblage that developed during crenulation formation consisted of garnet overgrowths, higher-Ca plagioclase overgrowths, phengitic muscovite, matrix biotite, ilmenite, and quartz. Compositions of these phases were measured on the microprobe using the compositional maps as location guides, and with the thermodynamic database and software of Berman (1991), were used to estimate syn-D_3 metamorphic conditions (Fig. 8a, b). Data from the fold hinge and fold limb domains of sample MT-1 (Fig. 2) yield consistent results of 600–650°C and 1.1 GPa (11 kbar). This consistency further supports the textural observation that both hinge and limb domains were tectonically active during crenulation cleavage formation. Further, the nearly identical P–T conditions estimated from distinct S_2 compositional layers within the Moretown Formation emphasize that detailed timing constraints can substantially reduce scatter in P–T calculations, and thus strengthen tectonic interpretations.

5. Discussion

5.1. Metamorphic reactions

Mineral assemblages in the Moretown schist at the end of the D_2 deformation probably included muscovite, biotite, chlorite, garnet, quartz, albitic plagioclase, ilmenite, and epidote. All of these phases are strongly aligned with the S_2 foliation, and all are at least locally deformed by D_3 crenulations. Chlorite generally occurs as large, cross-cutting, undeformed crystals, but some fine chlorite is aligned with S_2 and deformed around F_3 folds. Garnet porphyroblasts also contain abundant, very fine grained (~10–30 μm) inclusions of epidote. No epidote has been recognized in the matrix.

The D_3 (crenulation-producing) event involved the growth of Ca-richer plagioclase (oligoclase), phengitic muscovite, ilmenite, biotite, and minor amounts of garnet. Phases consumed are less well resolved by compositional maps, but probably include epidote, chlorite, quartz, biotite, and albitic plagioclase. Plagioclase composition jumped from albite (An_{03}) to oligoclase (An_{14-16}) during crenulation formation. Because diffusion is extremely slow in plagioclase, this jump represents the growth of new plagioclase on older plagioclase. The compositional gap corresponds to the peristerite miscibility gap in the plagioclase system (Fig. 8c). The Ca-rich side of the peristerite gap is typically observed to occur at approximately An_{22}, but peak temperatures in the Moretown Formation (600°C) were probably near the narrow upper part of the peristerite solvus (Smith, 1983). The corresponding loss of epidote from the assemblage suggests that Ca-richer plagioclase may have developed from a reaction such as (abbreviations after Kretz, 1983)

$$\mathrm{Ab + Ep + Qtz + Ms + Chl(+Bt)} = \mathrm{Pl(Ca\text{-}richer) + Grt(+Phengite) + H_2O} \quad (1)$$

and one balanced whole-rock reaction with compositions from the Moretown Formation is

$$\mathrm{1.0Ab + 0.1Ep + 0.15Qtz + 0.1Ms + 0.05Chl} = \mathrm{1.15Pl(Ca\text{-}richer) + 0.01Grt + 0.08Bt + H_2O.} \quad (2)$$

The exact form and stoichiometry of the reactions are currently under investigation, and depend on the specific behavior of Al-bearing phases such as chlorite, biotite, phengite, and garnet. Also, it is possible that some of the calcium (needed for the Ca-richer plagioclase) came from carbonate-bearing beds in the Moretown Formation but no such beds have yet been recognized in the study outcrop. Fig. 8(d) shows the location of four possible reactions, three of which are calculated equilibria based on the compositions in sample MT-1. The fourth represents a similar reaction experimentally investigated by Newton (1966) (see also Crawford, 1966). The locations of these reactions are consistent with estimated P–T conditions for D_3 deformation (Fig. 8d) and further demonstrate the internal consistency that can be achieved by combining structural and metamorphic timing data.

Phengitic muscovite may have developed from one of several reactions (Velde, 1965; Dempster, 1992). The synchronous growth of garnet and the consumption of biotite during D_3 suggests that one or both of the following may be involved

$$\mathrm{1.0Chl + 4.6Qtz = 0.7Phen + 0.95Grt + H_2O} \quad (3)$$

$$\mathrm{1.0Bt + 0.04Qtz = 0.36Phen + 0.54Grt(+Ilm).} \quad (4)$$

Metamorphic reactions such as those inferred for the Moretown Formation have important implications for mass transfer during crenulation cleavage formation. Compositional mapping indicates that, in addition to quartz, albite was an important component of the pre-D_3 (pre-crenulation) Moretown schists. Reaction (1) consumes albite, and all reactions noted above (and most other zoisite-consuming or phengite-producing reactions) consume quartz. Thus, some proportions of the dissolved materials were consumed during metamorphic reactions and are now present in the form of product phases such as phengite and oligoclase. The addition of new phengitic muscovite further increases

the mica to quartz ratio in crenulation limbs, thereby increasing the sense that components have been removed.

Petrologic analysis is currently underway to model the reaction history of the Moretown Formation. However, we have used simple mass balance calculations to model the importance of reactions such as Reactions (2)–(4) for the mass transfer, cleavage formation process. Assuming that the starting rock (post-D_2) had 60% mica, 20% quartz, and 20% albite we have calculated the mass balance involved with producing the observed new plagioclase and phengitic muscovite. This type of calculation is admittedly speculative, but several first-order conclusions can be drawn. First, regardless of reaction stoichiometry or starting assumptions, a significant amount of albite is consumed in producing the observed oligoclase; in most calculations, the amount is similar to that of product oligoclase. If the albite is preferentially dissolved from fold limb domains, then virtually all of the starting albite could be consumed to produce the observed oligoclase. Second, the calculated material loss from most reactions is dominated by albite. Because of the small molar volume of quartz and the small stoichiometric coefficient of quartz in the reactions, a relatively small volumetric amount of quartz is consumed (generally less than 10% of the starting amount). Thus, although the reaction-based transfer is significant, it is difficult to account for all of the observed quartz dissolution by metamorphic reactions alone. We conclude that some amount of deformation-induced solution transfer is also involved to deplete quartz from crenulation limb (M) domains.

5.2. Role of deformation vs metamorphism in mass transfer processes

Many workers have speculated on the possible mechanisms that might lead to deformation-induced dissolution of quartz, particularly the relative roles of strain-induced and stress-induced processes (Marlow and Etheridge, 1977; Bell et al., 1986; Bell and Cuff, 1989). Metamorphic reactions have been suggested to play an increasing role at higher metamorphic grades (Gray, 1979; Gray and Durney, 1979). Crenulation cleavage in the Moretown Formation developed at relatively high grade (amphibolite facies), and the results presented here suggest that prograde metamorphic reactions did provide a component of the driving force for mass transfer. However, the role of deformation is also apparent. Some reaction products, particularly plagioclase, were preferentially deposited in crenulation hinge QF domains, although others, phengitic muscovite, were not so strongly partitioned. Also, the fine-grained and equant nature of albite cores in crenulation limb domains suggests that reactants may have been preferentially consumed in the crenulation limbs. Although reactions may control the overall chemical balance, deformation is clearly important in localizing the reactants and products in active sites.

Two types of structural controls might be considered for metamorphic reaction sites. Gray and Durney (1979) proposed a pressure–solution model for solution transfer in which variations in normal stress and mean stress in crenulation microfolds lead to dissolution, transport, and deposition down chemical potential gradients. Although this process was specifically proposed for lower-grade rocks, it might work in combination with metamorphic reactions at higher grades to slightly favor dissolution of reactants in crenulation limbs and precipitation of products in hinges. Alternatively, Bell et al. (1986) suggested a strain-based mechanism whereby crenulation limbs are characterized by greater simple shear to pure shear strain ratios and by higher total strains; hinges have greater pure shear strain and dilation. They postulated that micas are preferentially stable in crenulation limbs because of their greater ability to accommodate shear strain and that quartz and feldspar are preferentially deposited in dilational, pure-shear-dominated hinge zones.

Metamorphic reactions are expected to occur, to some degree, in all domains, particularly if a metamorphic fluid is present. This is clearly the case in the Moretown Formation where reactants and products were observed in all structural settings (Fig. 9): M domains, QF domains, and domains without crenulation cleavage. Only the relative proportions of minerals vary from setting to setting. If the kinetics of mineral dissolution and precipitation are sluggish, for a reaction such as Reaction (1), then either of the above mechanisms might favor a greater amount of removal of unstable reactant phases from high-strain M domains, and a greater rate of growth of new product phases in dilatant QF domains. We favor a strain-based model such as that of Bell et al. (1986) because stress differences are expected to be small at elevated metamorphic temperatures, although at lower grades, both deformation-induced mechanisms may operate in concert with metamorphic reactions.

6. Conclusions

Compositional mapping of matrix domains of crenulated Moretown schist documents that greater than 10% of Ca-richer plagioclase (oligoclase) has been added to QF domains during crenulation cleavage formation. Much smaller amounts, on the order of 1%, have been added to the mica-rich M domains. Even though significant amounts of new material have been added, the QF domains are still dominated by the pre-crenulation, S_2 cleavage. Individual plagioclase grains within this cleavage have been significantly coarsened, possibly during dilation of the crenulation hinges, but the general orientation of the S_2 foliation remains (Fig. 9b). In these rocks, QF domains cannot be taken as representative of the character of the pre-crenulation texture. They are not windows to an earlier fabric state, but instead have been significantly modified during the crenulation forming event. Similarly, significant amounts of phengitic muscovite have grown or recrystallized in M domains (Fig. 9b). This tends to increase the contrast

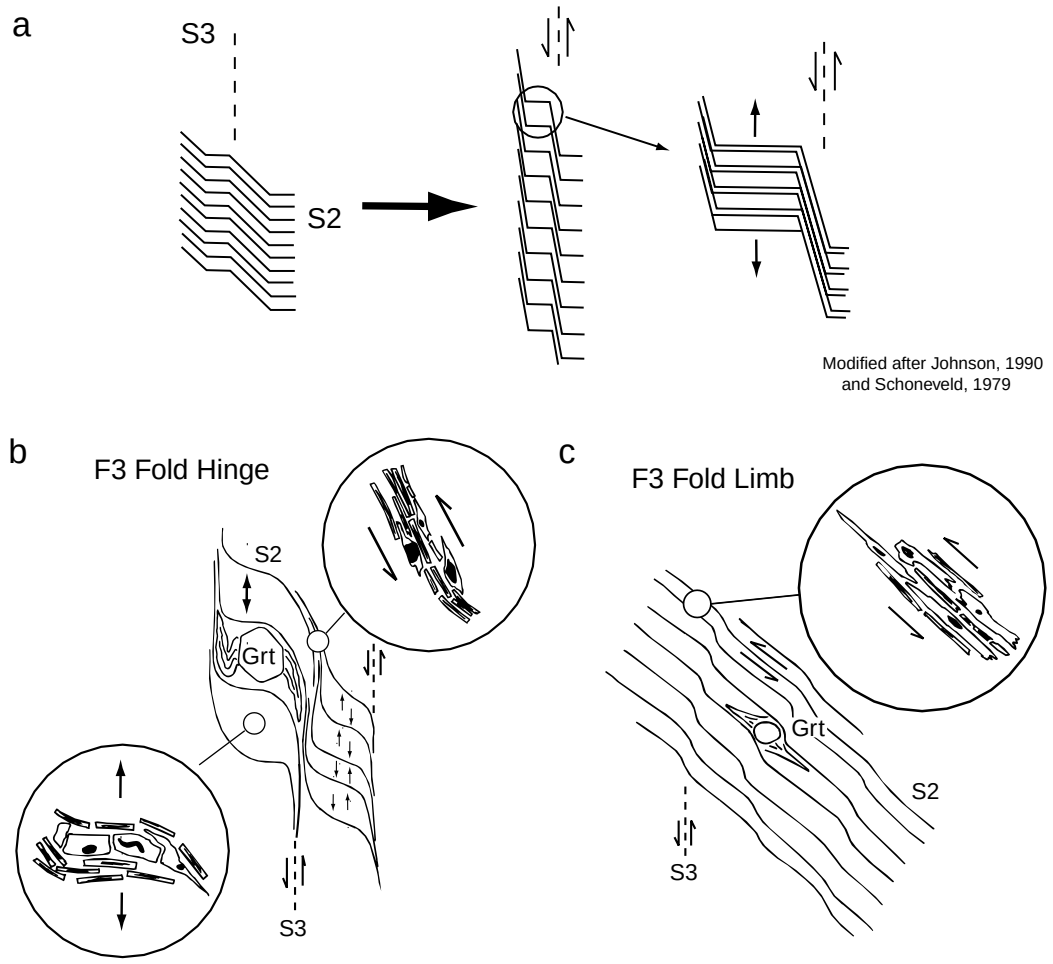

Fig. 9. Models for mass transfer during crenulation cleavage development. (a) Development of cleavage through dilation of QF domains and extension of M domains (modified after Johnson, 1990 and Schoneveld, 1979). (b) Close-up sketch of crenulation cleavage in the Moretown Formation. New plagioclase is added as overgrowths during dilation of QF domains; Ca-richer plagioclase and phengitic muscovite grow in M domains during shearing and extension. (c) Close-up sketch of S_2 cleavage in uncrenulated limb domains. Ca-richer plagioclase and phengitic muscovite are added as synkinematic overgrowths during reactivation of S_2 cleavage.

between limb and hinge domains and increase the sense of dissolution and volume loss from these domains.

Uncrenulated domains (F_3 fold limbs) in the Moretown Formation also show evidence of additions of second-generation plagioclase. Textures of plagioclase overgrowths indicate that the S_2 fabric was actively deforming during deposition of new plagioclase (Fig. 9c). The crenulation event has apparently reactivated the older S_2 fabric rather than forming a new crenulation cleavage. These uncrenulated domains are by no means undeformed domains, or windows to earlier fabric states, with which the crenulated domains can be compared. Any such comparison would only reveal the relative textural and compositional differences between domains deformed by distinct deformational processes.

Crenulation cleavage in the Moretown Formation results from an intimate interaction of microstructural processes and prograde metamorphic reactions. Processes such as pressure solution or strain solution may be important in localizing the reactants and products (Gray, 1979; Bell et al., 1986) but the mass transfer may be largely controlled by metamorphic reactions. Gray (1979) suggested that this sort of metamorphic interaction may be more characteristic of high-grade cleavages such as that in the Moretown Formation, but it seems possible that high-resolution compositional maps of lower-grade cleavages may reveal similar effects and a new appreciation of the role of metamorphic reactions in those rocks too.

Finally, it is important to note that the results of this study do not resolve, but instead probably complicate interpretations of bulk volume change during cleavage formation. They do verify that minerals are precipitated locally during cleavage formation, as suspected by many workers (Marlow and Etheridge, 1977; Gray and Durney, 1979; Mancktelow, 1994), and thus are not inconsistent with closed system behavior (assuming that sufficient early epidote was present). However, they also indicate that the cleavage-forming process involves a multi-component and multi-mineral mass transfer, implying that bulk geochemical evidence for volume loss may be subtle. Most importantly,

the results demonstrate that compositional maps represent a new tool for linking metamorphic petrology with microstructure and geochemistry. Quantitative metamorphic modeling techniques (e.g. Spear and Peacock, 1989) can be applied to discrete microstructural domains in order to constrain the complete metamorphic mass balance during a particular deformation, and the addition of microstructural timing constraints to metamorphic models will lead to more precise pressure–temperature–time–deformation models for orogenic rocks.

Acknowledgements

This research has been supported by NSF Grant 9725380. Partial graduate support for K. Scheltema was provided by the Isenberg Foundation. The electron microprobe was purchased with partial support from NSF Grant 88-16259, and NSF Grant 9503054 provided partial support for upgrading the mapping and analytical capability of the instrument. The authors sincerely thank Wouter Bleeker and Marc St Onge for their careful positive reviews of an earlier version of this manuscript.

References

Bell, T.H., Cuff, C., 1989. Dissolution, solution transfer, diffusion versus fluid flow and volume loss during deformation/metamorphism. Journal of Metamorphic Geology 7, 452–457.

Bell, T.H., Rubenach, M.J., Fleming, P.D., 1986. Porphyroblast nucleation, growth, and dissolution in regional metamorphic rocks as a function of deformation partitioning during foliation development. Journal of Metamorphic Geology 4, 37–67.

Berman, R.G., 1991. Thermobarometry using multi-equilibrium calculations: a new technique, with petrological applications. Canadian Mineralogist 29, 833–855.

Beutner, E.C., Charles, E.G., 1985. Large volume loss during cleavage formation, Hamburg Sequence, Pennsylvania. Geology 13, 803–805.

Borradaile, G.J., Bayly, M.B., Powell, C.M., 1982. Atlas of Deformational and Metamorphic Rock Fabrics. Springer, Berlin.

Cosgrove, J.W., 1976. The formation of crenulation cleavage. Journal of the Geological Society of London 132, 155–178.

Crawford, M.L., 1966. Composition of plagioclase and associated minerals in some schists from Vermont, U.S.A. and South Westland, New Zealand, with inferences about the peristerite solvus. Contributions to Mineralogy and Petrology 13, 269–294.

Dempster, T.J., 1992. Zoning and recrystallization of phengitic micas: implications for metamorphic equilibration. Contributions to Mineralogy and Petrology 109, 526–537.

Erslev, E.A., 1998. Limited, localized nonvolatile element flux and volume change in Appalachian slates. Geological Society of America Bulletin 110, 900–915.

Florence, F.P., Bayly, M.B., Menard, T., 1989. Localized variation in chemical partitioning in garnet; evidence for differential stress during metamorphism. Geological Society of America Abstracts with Programs 20, 20.

Goldstein, A., Knight, J., Kimball, K., 1998. Deformed graptolites, finite strain and volume in rocks of the taconic slate belt, New York and Vermont, USA. Journal of Structural Geology 11, 1769–1781.

Goldstein, A., Pickens, J., Klepeis, K., Linn, F., 1995. Finite strain heterogeneity and volume loss in slates of the Taconic Allocthon, Vermont, USA. Journal of Structural Geology 17, 1207–1216.

Gray, D.R., 1977aa. Morphologic classification of crenulation cleavage. Journal of Geology 85, 229–235.

Gray, D.R., 1977bb. Differentiation associated with discrete crenulation cleavages. Lithos 10, 89–101.

Gray, D.R., 1979. Microstructure of crenulation cleavages: an indicator of cleavage origin. American Journal of Science 279, 97–128.

Gray, D.R., Durney, D.W., 1979. Crenulation cleavage differentiation: implications of solution-deposition processes. Journal of Structural Geology 1, 73–80.

Gresens, R.L., 1967. Composition–volume relationships of metasomatism. Chemical Geology 2, 47–65.

Hatch, N.L.J., 1969. Geologic map of the Worthington quadrangle, Hampshire and Berkshire counties, Massachusetts. United States Geological Survey, Washington, DC.

Hatch, N.L.J., Schnabel, R.W., Norton, S.A., 1968. Stratigraphy and correlation of the rocks on the east limb of the Berkshire Anticlinorium in western Massachusetts and north-central Connecticut. In: Zen, E.A. (Ed.). Studies of Appalachian Geology, Northern and Marine. Interscience, New York, pp. 117–184.

Johnson, S.E., 1990. Lack of porphyroblast rotation in the Otago schists, New Zealand: implications for crenulation cleavage development, folding and deformation partitioning. Journal of Metamorphic Geology 8, 13–30.

Karabinos, P., Williamson, B.F., 1994. Constraints on the timing of Taconian and Acadian deformation in western Massachusetts. Northeastern Geology 16, 1–8.

Kretz, R., 1983. Symbols for rock-forming minerals. American Mineralogist 68, 277–279.

Mancktelow, N.S., 1994. On volume change and mass transport during the development of crenulation cleavage. Journal of Structural Geology 16, 1217–1231.

Marlow, P.C., Etheridge, M.A., 1977. Development of a layered crenulation cleavage in mica schists of the Kanmantoo group near Macclesfield, South Australia. Geological Society of America Bulletin 97, 354–368.

Newton, R.C., 1966. Some calc–silicate equilibrium reactions. American Journal of Science 264, 204–222.

Passchier, C.W., Trouw, R.A.J., 1996. Microtectonics. Springer, Berlin.

Pattison, D.R.M., Bégin, N.J., 1994. Zoning patterns in orthopyroxene and garnet in granulites: implications for geothermometry. Journal of Metamorphic Geology 12, 387–410.

Potdevine, J.L., Marquer, D., 1987. Methodes de quantification des transferts de matiere par les fluides dans les roches metamorphiques deformees. Geodinamica Acta 1, 193–206.

Ratcliffe, N.M., Walsh, G.J., Aleinikoff, J.N., 1997. Basement, metasedimentary, and tectonic cover of the Green Mountain Massif and western flank of the Chester Dome. In: Grover, T.W., Mango, H.N., Hasenohr, E.J. (Eds.). New England Intercollegiate Geological Conference, Guidebook to Field Trips in Vermont and Adjacent New Hampshire and New York. Castleton State College, Castleton.

Robinson, P., Ratcliffe, N.M., Hepburn, J.S., 1993. A new tectonic–stratigraphic transect across the New England Caledonides of Massachusetts. In: Cheney, J.T., Hepburn, J.C. (Eds.). Geological Society of America, Field Trip Guidebook for the Northeastern United States. University of Massachusetts, Amherst.

Saha, D., 1998. Local volume change vs overall volume constancy during crenulation cleavage development in low grade rocks. Journal of Structural Geology 20, 587–599.

Scheltema, K.E., 1996. Mass movement and volume change during late deformation and crenulation cleavage formation in the Moretown Formation, Massachusetts. Undergraduate thesis, Hampshire College.

Scheltema, K.E., Williams, M.L., 1998. Microstructural and compositional constraints on a geochemically based estimate of volume loss in the Moretown Fm., Western Massachusetts: new twist in an old mystery. Geological Society of America Abstracts with Programs 30, 235.

Scheltema, K.E., Williams, M.L., 1999. Microfabric and micro-compositional analysis of the Moretown Formation, West Cummington,

Massachusetts. Geological Society of America Abstracts with Programs 31.

Schoneveld, C., 1979. The geometry and significance of inclusion patterns in syntectonic porphyroblasts. Ph.D. thesis, University of Leyden.

Smith, J.V., 1983. Phase equilibria of plagioclase. In: Ribbe, P.H. (Ed.). Feldspar Mineralogy. 2nd ed. Reviews in Mineralogy, vol. 2. Mineralogical Society of America, pp. 223–240.

Spear, F.S., Kohn, M.J., 1996. Trace element zoning in garnet as a monitor of crustal melting. Geology 24, 574–577.

Spear, F.S., Peacock, S.M., 1989. Short Course in Geology, vol. 7. American Geophysical Union, Washington, DC.

Stanley, R.S., Hatch, N.L.J., 1985. The pre-Silurian geology of the Rowe–Hawley zone. The Bedrock Geology of Massachusetts: US Geological Survey Professional Paper 1366, pp. A1–A39.

Stanley, R.S., Ratcliff, N.M., 1985. Tectonic synthesis of the Taconian orogeny in western New England. Geological Society of America Bulletin 96, 1227–1250.

Stanley, R.S., Roy, D.L., Hatch, N.L.J., Knapp, D.A., 1984. Evidence for tectonic emplacement of ultramafic and associated rocks in the pre-Silurian eugeoclinal belt of western New England; vestiges of an ancient accretionary wedge. American Journal of Science 284, 559–595.

Tan, B.K., Gray, D.R., Stewart, I., 1995. Volume change accompanying cleavage development in Graptolitic shales from Grisborne, Victoria, Australia. Journal of Structural Geology 17, 1387–1394.

Thompson, J.B.J., Rosenfeld, J.L., Chamberlain, C.P., 1993. Sequence and correlation of tectonic and metamorphic events in southeastern Vermont. In: Cheney, J.T., Hepburn, J.C. (Eds.). Geological Society of America, Field Trip Guidebook for the Northeastern United States. University of Massachusetts, Amherst.

Velde, B., 1965. Phengite micas: synthesis, stability, and natural occurrence. American Journal of Science 263, 886–913.

Waldron, H.M., Sandiford, M., 1988. Deformation volume and cleavage development in metasedimentary rocks from the Ballarat slate belt. Journal of Structural Geology 10, 53–62.

Williams, M.L., 1994. Sigmoidal inclusion trails, punctuated fabric development and interactions between metamorphism and deformation. Journal of Metamorphic Geology 12, 1–21.

Wright, T.O., Henderson, J.R., 1992. Volume loss during cleavage formation in the Meguma Group, Nova Scotia, Canada. Journal of Structural Geology 14, 281–290.